Calcium Binding Decreases the Stokes Radius of Calmodulin and Mutants R74A, R90A, and R90G

Brenda R. Sorensen and Madeline A. Shea
Department of Biochemistry, University of Iowa College of Medicine, Iowa City, Iowa 52242-1109 USA

ABSTRACT Calmodulin (CaM) is an intracellular cooperative calcium-binding protein essential for activating many diverse target proteins. Biophysical studies of the calcium-induced conformational changes of CaM disagree on the structure of the linker between domains and possible orientations of the domains. Molecular dynamics studies have predicted that Ca_4^{2+}CaM is in equilibrium between an extended and compact conformation and that Arg74 and Arg90 are critical to the compaction process. In this study gel permeation chromatography was used to resolve calcium-induced changes in the hydrated shape of CaM at pH 7.4 and 5.6. Results showed that mutation of Arg74 to Ala increases the R_s as predicted; however, the average separation of domains in Ca_4^{2+}-CaM was larger than predicted by molecular dynamics. Mutation of Arg90 to Ala or Gly affected the dimensions of apo-CaM more than those of Ca_4^{2+}-CaM. Calcium binding to CaM and mutants (R74A-CaM, R90A-CaM, and R90G-CaM) lowered the Stokes radius (R_s). Differences between R_s values reported here and R_g values determined by small-angle x-ray scattering studies illustrate the importance of using multiple techniques to explore the solution properties of a flexible protein such as CaM.

INTRODUCTION

Calmodulin (CaM) (Fig. 1) is the primary intracellular receptor for calcium, binding four calcium ions cooperatively (Crouch et al., 1980; Cox, 1988; Wang, 1985). Calcium binding exposes hydrophobic surfaces in each domain (LaPorte et al., 1980). Structures of Ca_4^{2+}-CaM have been determined by x-ray diffraction (XRD) (Babu et al., 1985, 1988; Taylor et al., 1991; Chattopadhyaya et al., 1992) and NMR (Ikura et al., 1991; Barbato et al., 1992). These approaches have resolved similar structures for both domains which contain two helix-loop-helix sequences (EF-hand; see Fig. 2). Each site consists of a sequence of 12 residues; five residues directly chelate the calcium ion (their positions are designated X, Y, Z, $-Y$, $-X$, and $-Z$ (Kretsinger et al., 1973; cf. Strynadka et al., 1989; see Fig. 1). The helices flanking the four binding sites are designated by letters (e.g., helices E and F flank site III; see Fig. 2).

A controversy over structures adopted by Ca_4^{2+}-CaM has arisen because XRD studies showed the domains separated by a seven-turn α-helix (Babu et al., 1988), whereas NMR showed this helix to be disrupted by four nonhelical residues from D78 to S81 (Ikura et al., 1991). The NMR studies are consistent with earlier chemical studies suggesting that the domains are connected by a "flexible tether" (Persechini et al., 1988; see Kretsinger, 1992, for a review) that allows variable orientation of the two domains relative to each other. Small-angle x-ray scattering studies (Heidorn and Trewhella, 1988, 1990; Matsushima et al., 1989; Kataoka et al., 1989, 1991a) and fluorescence studies (Small and Anderson, 1988; Yao et al., 1994) of CaM suggest that the central helix is not rigid under all solution conditions. This is expected to be critical to the physiological roles of CaM.

CaM serves as a second messenger in signal transduction pathways via interactions with many distinct target proteins (cf. Klee and Cohen, 1988) and plays an essential role in the regulation of varied processes such as cell cycle progression, cell motility, and contraction (Lu and Means, 1993; Lu et al., 1993; Davis et al., 1986; Rasmussen et al., 1990; Rasmussen and Means, 1989). Structures resolved for CaM-target complexes show the two domains of CaM in close proximity, with equivalent interactions with the target (see Crivici and Ikura, 1995, for a review).

However, compact structures are possible in the absence of "cross-linking" afforded by a target peptide. A crystallographic study of Ca_4^{2+}-CaM with one molecule of TFP bound (only to the C-terminal domain) showed the two domains in close proximity (Cook et al., 1994). Functional studies of *Paramecium* CaM (Kung et al., 1992) and chimeric CaM (George et al., 1993) support differential roles of the sites and domains. Functional energetic studies of site-knockout mutants (Maune et al., 1988, 1992) and wild-type CaM (Pedigo and Shea, 1995; Shea et al., 1996) have indicated that even in the absence of target protein, the two domains of CaM interact over the course of binding four calcium ions. Thus, despite detailed structural studies of Ca_4^{2+}-CaM bound to target peptides or drugs and increasingly fine dissection of the roles of individual sites of CaM in enzyme activation, many aspects of the molecular mechanism of CaM function are not understood.

The controversy over the structural nature of the linker between domains and the apparent dynamic variability of the structure of CaM in solution prompted a series of molecular dynamics studies (Mehler et al., 1991; Pascual-Ahuir et al., 1991; Weinstein and Mehler, 1994) to explore how this flexibility might be controlled. The simulations

Received for publication 14 August 1996 and in final form 17 September 1996.

Address reprint requests to Madeline A. Shea, Department of Biochemistry, University of Iowa College of Medicine, Iowa City, IA 52242-1109. Tel.: 319-335-7885; Fax: 319-335-9570; E-mail: madeline-shea@uiowa.edu.

0006-3495/96/12/3407/14 $2.00

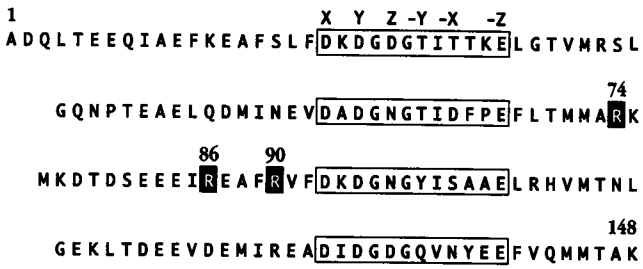

FIGURE 1 Amino acid sequence of rat CaM divided into four segments. Residues 1–39 include site I; residues 40–75 include site II; residues 76–112 include site III; residues 113–148 include site IV. The 12 residues comprising each calcium-binding site (*boxed residues*) are aligned, and those involved in chelating calcium ion are in positions *X*, *Y*, *Z*, $-Y$, and $-Z$. The arginine residues (R) implicated in a model for a ratcheting mechanism of compaction of CaM are in shaded boxes.

started with Ca_4^{2+}-CaM in the conformation of 3cln (Babu et al., 1988) and included water molecules in addition to those observed crystallographically. The family of simulated structures suggested that calcium-saturated CaM would adopt a compact conformation with a computed radius of gyration (R_g) of 17 Å (Mehler et al., 1991; Pascual-Ahuir et al., 1991), ~5 Å smaller than that of 3cln (Table 1). Comparison of the pair distribution functions computed for these models (called CaM2 and CaM10) and those obtained experimentally for Ca_4^{2+}-CaM using small-angle x-ray scattering studies (Heidorn and Trewhella, 1988, 1990; Kataoka et al., 1989, 1991a; Matsushima et al., 1989) suggested that CaM2 and CaM10 were as compact as Ca_4^{2+}-CaM complexed to mastoparan (Matsushima et al., 1989) or melittin (Kataoka et al., 1989, 1991a), where both domains of CaM

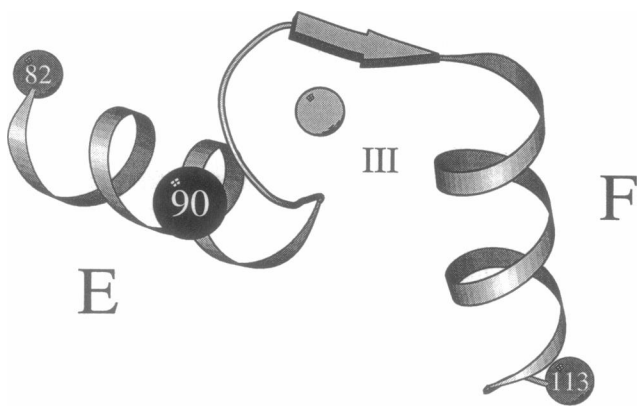

FIGURE 2 Ribbon drawing (Kraulis, 1991) of the α-carbon backbone of the E and F helices flanking calcium-binding site III in the C-terminal domain of the crystallographic structure of Ca_4^{2+}-CaM (Babu et al., 1988). Coordinates were taken from the Brookhaven Protein Data Bank file 3cln.pdb (Bernstein et al., 1977; Abola et al., 1987). The calcium ion in site III appears as a shaded sphere. The first and last residues in this fragment are also highlighted with shaded spheres numbered 82 and 113, respectively. Arginine 90 has been proposed to be critical for the compaction of Ca_4^{2+}-CaM (Pascual-Ahuir et al., 1991; Weinstein and Mehler, 1994) and is indicated with a blackened sphere.

TABLE 1 Size and shape of Ca_4^{2+}-CaM and globular proteins

	M_w*	R_g (Å)#	R_s (Å)§
Calmodulin structures			
WT (3cln)	16.7	21.91	23.95
WT (CaM10)	16.7	16.99	NA
R74A model	16.6	24.02	24.26
R90A model	16.6	24.32	24.02
Globular proteins			
Cytochrome C	12.4¶	13.07	16.3¶
Ribonuclease A	13.7‖	14.20	16.4‖
Chymotrypsinogen A	25.0‖	16.19	22.4‖
Carbonic anhydrase	29.0¶	17.37	20.1¶

*The molecular weight for the calmodulin structures was calculated based on the amino acid sequence.
#R_g was calculated using HYDRO (Garcia de la Torre & Bloomfield, 1981; Garcia de la Torre *et al.*, 1994). The R_s values reported were either §determined experimentally using gel permeation chromatography (no value is reported for CaM10 because it is a theoretical model of WT CaM), or were taken from ¶(Potschka, 1987) or ‖(Pharmacia LKB Biotechnology, 1991.).

interact with the target peptide. Using the R_g value reported for Ca_4^{2+}-CaM complexed to mastoparan (Matsushima et al., 1989) and the R_g for CaM2, it was estimated that almost 30% of the populated species of Ca_4^{2+}-CaM in solution could be this compact (Mehler et al., 1991), with the balance being as extended as 3cln (Babu et al., 1988).

Fig. 3, *A* and *B*, illustrates the differences in the backbone conformations of 3cln and the simulated model CaM10. Weinstein and co-workers described the orientation of the domains by a change in the dihedral angle between the four calcium ions (Pascual-Ahuir et al., 1991), as depicted below.

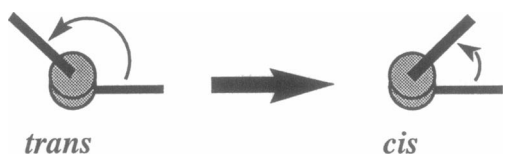

SCHEME 1

The circles represent calcium ions in sites II and III of CaM, and the lines are drawn to calcium ions in sites I and IV. In CaM10, before compaction, the relative orientation of the N- and C-terminal domains has changed from *trans*, as was observed in 3cln, to *cis*. The "ratcheting" compaction of Ca_4^{2+}-CaM seen in the trajectory of CAM10 appeared to depend on a changing network of hydrogen bonds; the principal residues were three arginine side chains (Arg74, Arg90, and, to a lesser extent, Arg86) interacting with residues up to 20 amino acids away in the CaM sequence (Pascual-Ahuir et al., 1991; Weinstein and Mehler, 1994).

In Fig. 4, Arg74, Arg90, and their proposed interacting residues in the rat CaM sequence were compared to 42 other sequences of CaM. This showed that 1) 93% of these sequences contained an arginine residue at position 74, 2) 64% contained arginine at position 90 (with an additional

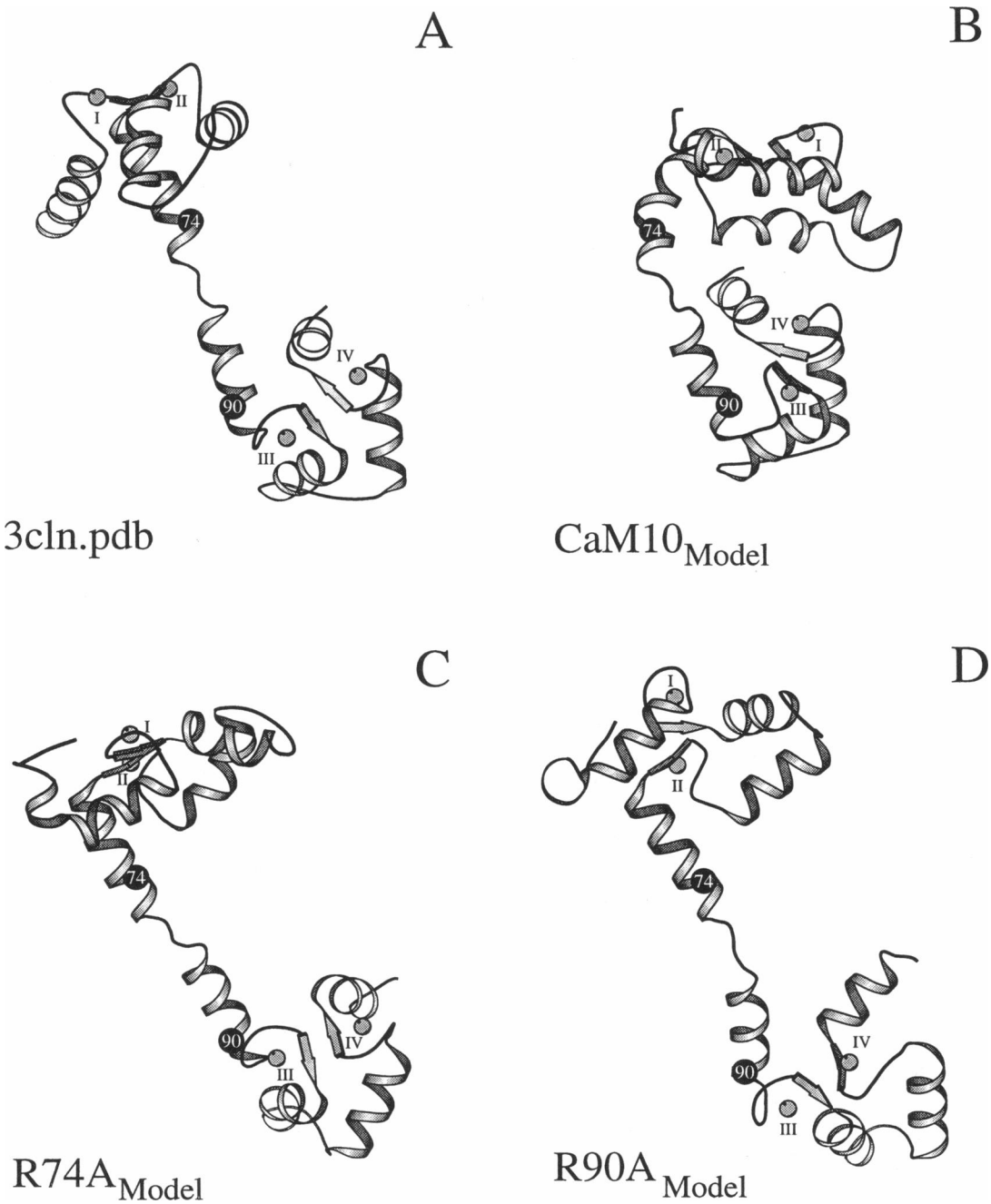

FIGURE 3 Ribbon drawings (Kraulis, 1991) of the α-carbon backbone of (*A*) 3cln.pdb, a crystallographic structure of Ca_4^{2+}-CaM (Babu et al., 1988), in which residues 5–147 were resolved; (*B*) CaM10, an energy-minimized model of Ca_4^{2+}-CaM (Pascual-Ahuir et al., 1991; Weinstein and Mehler, 1994); (*C*) an energy-minimized model of CaM10 with alanine substituted for the arginine at position 74; and (*D*) an energy-minimized model of CaM10 with alanine substituted for the arginine at position 90. Coordinates for 3cln.pdb were taken from the Brookhaven Protein Data Bank (Bernstein et al., 1977; Abola et al., 1987). The energy-minimized models in *B–D* were determined using molecular dynamics simulations with 3cln.pdb as the starting structure (Pascual-Ahuir et al., 1991; Weinstein and Mehler, 1994). Arginines 74 and 90 are indicated with dark spheres. The four calcium-binding sites in CaM are illustrated as roman numerals I–IV, with calcium ions appearing as shaded spheres. The secondary structure type of the junction of the helix leading out of site II (helix D) and the helix leading into site III (helix E) is based on NMR studies of Ca_4^{2+}-CaM in solution (Ikura et al., 1991). The secondary structure types depicted in CaM10 were determined using Procheck (Laskowski et al., 1993); identical structures are depicted in the models of R74A and R90A for comparison.

33% containing a conservative lysine substitution), and 3) 43% contained an arginine residue at position 86 (with an additional 41% containing a lysine). The high degree of conservation of Arg74 and Arg90 supported the proposal that they are important for the structure and function of CaM.

To explore theoretically the role of Arg74, Arg 86, and Arg90 in compaction, an alanine was substituted computa

rat CaM:	E54	V55	T70	**R74**	E83	E87	**R90**	G96	N97
Type H-bond:	CO	CO	OG1		OE1	OE1		CO	CO
	E:42	V:39	T:21	**R:39**	E:39	E:42	**R:27**	G:26	N:37
		I: 2	N:13	**K: 3**	A: 1		**K:14**	Q:13	D: 5
		A: 1	S: 4		D: 1		**Q: 1**	N: 2	
			E: 1		K: 1			S: 1	
			G: 1						
			M: 1						
			V: 1						

FIGURE 4 An illustration of the sequence homology for Arg74, R90 (*in bold*) and their interacting residues as proposed (Pascual-Ahuir et al., 1991; Weinstein and Mehler, 1994). The 42 sequences most homologous to rat CaM were compared using FASTA (GCG, Madison, WI) searching the Swiss Protein database. The residues found in the 42 sequences at the positions indicated and their frequency are reported below the corresponding CaM residue. The type of hydrogen bonding interaction between Arg74 or Arg90 and these residues is also indicated where Glu54, Val55, and Thr70 hydrogen bond with Arg74; and Glu83, Glu87, Gly96, and Asn97 hydrogen bond to Arg90.

tionally for an arginine (Weinstein and Mehler, 1994). Simulations for the R86A model yielded a compact structure similar to that of CaM10. The largest deviation from CaM10 had been predicted for the R74A model because Arg74 in wild-type CaM was involved in a hydrogen bonding interaction with at least two residues at all times during the simulation leading to CAM10 (Weinstein et al., 1994). The R74A model and R90A model are depicted in Fig. 3, *C* and *D*. The model structures were more extended than 3cln (their starting structure; Weinstein and Mehler, 1994) and had dihedral angles (per Eq. 1) smaller than that of 3cln ($-134°$); the R90A model ($-43°$) deviated the most, and CaM10 ($-72°$) and the R74A model ($-77°$) were similar (Weinstein and Mehler, 1994) in this respect.

The goal of the present study was to explore the calcium-induced conformational changes in CaM and determine experimentally whether changes at Arg74 and Arg90 would detectably alter the structural diversity of Ca_4^{2+}-CaM. For the sake of direct comparison with the computational studies (Weinstein and Mehler, 1994), CaM was mutated to have an alanine substituted for Arg74 (R74A-CaM) or Arg90 (R90A-CaM). Because of the helical propensity of alanine, these changes were expected to be consistent with the computational models suggesting more extended structures. Thus Arg90 was also substituted by glycine (R90G-CaM) to test for the effect of introducing a "helix-breaking" residue near the flexible tether in CaM. The hydrodynamic behavior of these proteins has been studied using gel permeation chromatography (GPC) at pH 7.4 and pH 5.6 and compared to effects predicted by the molecular dynamics simulations discussed above (Pascual-Ahuir et al., 1991; Weinstein and Mehler, 1994).

MATERIALS AND METHODS

Mutagenesis

Recombinant rat CaM was overexpressed in *E. coli* using the T7-7 vector (Tabor and Richardson, 1985) in Lys-S cells (U.S. Biochemicals, Cleveland, OH) as described previously (Pedigo et al., 1995). Recombinant CaM differs from tissue-derived CaM in that the N-terminus is unacetylated and K115 is not trimethylated. Mutations of CaM were created using a double-stranded DNA mutagenesis kit available from CLONTECHnique (no. K1600-1; Palo Alto, CA). Three primers were synthesized by the DNA Facility of the Diabetes and Endocrinology Research Center, University of Iowa College of Medicine (Iowa City, IA). Primer A (5′-GAAGAAAT-TAGAGAGGCCTTCGCCGTGTTG-3′) was designed to mutate Arg90 (-**CGT**-) to alanine (-**GCC**-). Primer B (5′-GAAATTAGA GAGGCCT-TCGGTGTGTTG-3′) was designed to mutate Arg90 (-**CGT**-) to glycine (-**GGT**-). Primer C (5′-CTGACAATGATGGCCGCAAAAATGAA-3′) was designed to mutate Arg74 (-**AGA**-) to alanine (-**GCA**-). These primers also introduced a unique restriction enzyme recognition site (*Stu*I or *Eae*I) used to screen the mutated plasmids. In the primer sequences above, the mutated codon is in bold and the *Stu*I and *Eae*I recognition sites are underlined. Mutations were confirmed by 5′ and 3′ DNA sequencing (DNA Facility of the Diabetes and Endocrinology Research Center, University of Iowa College of Medicine, Iowa City, IA).

Protein purification

The recombinant wild-type CaM, R74A-CaM, R90A-CaM, and R90G-CaM were purified using phenyl sepharose CL-4B (Pharmacia Biotech, Piscataway, NJ) chromatography (Putkey et al., 1985), to approximately 99% purity as judged by silver staining of overloaded reducing sodium dodecyl sulfate-polyacrylamide gel electrophoresis experiments and by small zone GPC on a Superdex75 column (Pharmacia Biotech) with the eluent monitored at 280 nm. Purified fractions were collected, pooled, and dialyzed in a buffer of 50 mM HEPES and 100 mM KCl (pH 7.40, 22°C); aliquots were stored at −20°C. Protein concentrations were determined using the BCA Protein Assay (catalog no. 23225; Pierce, Rockford, IL), which had been calibrated for CaM by comparison with amino acid analysis of wild-type (WT) CaM.

Chemical characterization

The expression of R74A-CaM, R90A-CaM, and R90G-CaM proteins was confirmed by amino acid analysis performed by the Protein Structure Facility (University of Iowa College of Medicine, Iowa City, IA). The data were normalized to the expected occurrence of at least four amino acids. Results for wild-type CaM were 5.91 mol Arg, 10.50 mol Ala, and 10.52 mol Gly, where 6 mol Arg, 11 mol Ala, and 11 mol Gly were expected. For the mutants having Ala substituted for Arg, 5 mol Arg and 12 mol Ala residues were expected per mole of protein; results for R90A-CaM were 5.12 mol Arg and 11.78 mol Ala residues, and for R74A-CaM were 4.95 mol Arg and 11.89 mol Ala residues. Amino acid analysis of R90G-CaM indicated that it contained 5.28 mol Arg and 12.38 mol glycine residues (5 and 12 were expected).

The bacterially expressed proteins were further characterized electrophoretically. Samples of CaM in buffer containing 5 mM EGTA or 5 mM $CaCl_2$ were run on 17% Tris-glycine polyacrylamide gels, and the expected calcium-induced increase in mobility was observed for WT CaM and all three of the mutants. Isoelectric focusing was performed on Isogel agarose IEF plates with a pH range of 3–10 (catalog no. 56011; FMC, Rockland, ME). Using the Genetics Computer Group software (GCG) (Madison, WI), we predicted the isoelectric point (pI) for all three mutant proteins to be 3.87; wild-type CaM was predicted to have a pI of 3.92. The experimentally resolved pI for R74A-CaM was 3.99, that of R90G-CaM was 3.97, and that of R90A-CaM and wild-type CaM were 4.06.

Preparation of calmodulin samples in pCa/pH buffers

Proteins (WT CaM, R74A-CaM, R90A-CaM, and R90G-CaM) were prepared to be calcium-saturated or apo at pH 7.4 and 5.6. They were saturated with calcium by the addition of concentrated $CaCl_2$ in buffer to a final

concentration of 4 mM $CaCl_2$ and diluted 10-fold with either buffer A (50 mM HEPES, 91 mM KCl, 0.5 mM EGTA, 0.5 mM nitrilotriacetic acid (NTA), and 5.2 mM $CaCl_2$ (pCa 2.84 ± 0.01), pH 7.41 at 23°C) or buffer B (50 mM piperazine-*N,N'*-bis(2-ethanesulfonic acid (PIPES), 89 mM KCl, 0.5 mM EGTA, 0.5 mM NTA, and 5.2 mM $CaCl_2$ (pCa 2.27 ± 0.01), pH 5.60, at 23°C) where pCa = $-\log[Ca^{2+}]_{free}$. CaM samples were depleted of calcium by the addition of EGTA to a final concentration of 0.5 mM at pH 7.4 or 5 mM at pH 5.6 and diluted 10-fold using either buffer C (50 mM HEPES, 91 mM KCl, 0.5 mM EGTA, 0.5 mM NTA (pCa 8.86 ± 0.18), pH 7.40) or buffer D (50 mM PIPES, 89 mM KCl, 0.5 mM EGTA, 0.5 mM NTA (pCa 6.64 ± 0.63), pH 5.61).

The experimental determination of the pCa of calcium buffers was described previously (Pedigo et al., 1995), and calcium titrations of WT CaM monitored by tyrosine fluorescence were performed in these buffers to ensure that CaM was completely saturated or depleted of calcium before the chromatographic studies (Sorensen and Shea, 1995, and data not shown). Stock CaM concentrations after dilution ranged from 10.2 μM for R90G-CaM to 2.1 μM for R90A-CaM. Each 250-μl sample contained 1 μl acetone as an internal standard used to normalize all elution profiles; studies in the absence of acetone demonstrated that acetone did not affect the elution behavior of any CaM (data not shown).

Small-zone gel permeation chromatography

Small-zone analytical GPC studies were conducted on a Basic Pharmacia FPLC system at room temperature (23 ± 1°C) using a Superdex 75 column (Pharmacia Biotech). The column was equilibrated with at least two column volumes of buffer A, B, C, or D described above. The elution profiles were monitored at 280 nm. The column characteristics were determined by the elution volumes for acetone and blue dextran. The column was calibrated by determining the elution volumes for the following globular proteins: bovine serum albumin (BSA), ovalbumin, chymotrypsin, and ribonuclease A (Pharmacia Biotech). Preparation of column standards (20 mg/ml) was as described for CaM samples, with the exception that the standards were diluted 20-fold to a final concentration of 1 mg/ml in each of the buffers.

All samples were filtered through 0.2-μm filters before loading 200 μl of CaM samples or 110 μl of the mixture of calibration standards onto the column at a flow rate of 0.4 ml/min. The values reported here are representative of more than 100 analyses that tested the effects of varying FPLC instrumentation and columns, temperature, and multiple buffer and protein preparations. The variability of column characteristics was minimal, as judged by consistent elution volumes for acetone, blue dextran, and column standards under all conditions tested. (No calcium-dependent behavior was observed for the column standards.) The precision of Stokes radius (R_s) values ranged from 0.1 to 0.2 Å. The results reported in the tables are averages of at least three trials for each protein sample run under identical conditions. There was no evidence for interactions of CaM with the resin under any conditions tested. CaM eluted as a symmetrical peak on either Superdex 75 (used for all studies reported) or Sephadex G-50. All elution volumes (retention times) were greater than expected for a protein of this mass; interactions would have caused retardation.

Analysis of R_s

The theory of protein separation by small-zone analytical GPC has been treated thoroughly (Porath, 1963; Laurent and Killander, 1964; Ackers, 1964, 1967, 1970; Andrews, 1964, 1965, 1970; Ackers and Thompson, 1965; Siegel and Monty, 1966; Henn and Ackers, 1969; Tanford et al., 1974). The elution behavior of a macromolecule may be described by the distribution coefficient (K_d; Andrews, 1970) or partition coefficient (σ; Ackers, 1967), which represents the fraction of the solvent volume within the gel matrix that is accessible to the macromolecule. The volume at which a macromolecule elutes from the column at maximum concentration is denoted as the elution volume (V_e) and is given by

$$V_e = V_o - \sigma \cdot V_i, \tag{2}$$

where V_o is the void volume (the solvent volume outside of the gel matrix measured by the elution of a macromolecule too large to enter the beads), and V_i is the internal volume that is the total volume accessible to solvent. Rearrangement of Eq. 2 gives the expression for the partition coefficient σ,

$$\sigma = (V_e - V_o)/V_i \tag{3}$$

which ranges in value from 0 to 1. The internal volume of a column is determined indirectly as the difference between the total solvent-accessible volume (V_s) of the column bed (as probed by a small molecule such as glycyl-glycine or acetone) and the void volume (probed by a totally excluded molecule such as blue dextran). Thus, $V_i = V_s - V_o$. The parameter σ is independent of variations in column bed preparation and dimensions.

Models for the separation of macromolecules by analytical GPC have been proposed based on different assumed geometries of the gel matrix (cf. Ogston, 1958; Squire, 1964). However, multiple independent approaches for describing elution behavior correlate equally well (see Ackers, 1970, for a review). A formulation of the relationship between Stokes radius and elution volume (given in Eq. 4) is based on the experimental observation that the distribution of solute-accessible volume within gel beads may be described by a Gaussian probability function (Ackers, 1967):

$$R_s = a_o + b_o \cdot \text{erfc}^{-1}\sigma, \tag{4}$$

where a_o and b_o are specific for a column and determined by fitting elution data for calibration standards of known R_s and experimentally determined partition coefficients, σ. Calibration values were 35.5 Å for BSA, 30.5 Å for ovalbumin, 20.9 Å for chymotrypsin, and 16.4 Å for ribonuclease A (Tanford et al., 1974; Pharmacia LKB Biotechnology, 1991); the void volume (V_o) was determined with blue dextran, and the solvent volume (V_s) was determined with acetone. Values of a_o and b_o were determined using nonlin (Johnson and Frasier, 1985) applied to the calibration data; values for the inverse error function complement were determined using the solver function in Microsoft Excel v.4.0.

Analysis of shape

The transport behavior of a macromolecule provides information about its shape. The translational frictional coefficient f_o of a spherical particle is related to fluid viscosity by Stokes' law (Eq. 5):

$$f_o = 6\pi\eta r_o, \tag{5}$$

where η is the viscosity of water at 20°C and r_o is the radius of the sphere. The frictional coefficient, f, for translation of a hydrodynamically equivalent nonspherical particle can be described according to Eq. 6:

$$f = 6\pi\eta R_s. \tag{6}$$

For a solvated sphere, the radius is given by Eq. 7

$$r_o = \left[\frac{3M_w\nu}{4\pi N}\left(1 + \frac{w}{\rho\nu}\right)\right]^{1/3}, \tag{7}$$

where M_w is the molecular weight, w is the hydration in grams of water bound per gram of protein, ρ is the density of water, ν is the partial specific volume of the macromolecule, and N is Avogadro's number (Andrews, 1970; Squire and Himmel, 1979; Stafford and Schuster, 1995). The frictional ratio is represented by

$$f/f_o = R_s \cdot \left[\frac{3M_w\nu}{4\pi N}\left(1 + \frac{w}{\rho\nu}\right)\right]^{-1/3} \tag{8}$$

(Stafford and Schuster, 1995). It should be noted that at least two conven

tions for this ratio are in use; f/f_o is often equated with f/f_{min}, where

$$f_{min} = 6\pi\eta r_{min} = 6\pi\eta\left[\frac{3M_w\nu}{4\pi N}\right]^{1/3}, \quad (9)$$

and r_{min} represents the radius of an unsolvated spherical particle with the same mass and partial specific volume as the protein under consideration (see Stafford and Schuster, 1995). Deviations of f/f_o from unity are indicative of a nonspherical molecular shape and the effects of hydration. To evaluate the contribution of the two factors, Oncley developed an approach that separated the frictional ratio into two terms: f/f_e, which relates to hydration, and f_e/f_o, which relates to asymmetry of molecular shape (Oncley, 1941). Using the Perrin formulas for the frictional ratio of ellipsoids (Perrin, 1936), values for f_e/f_o can be calculated given various axial ratios (a/b) of the ellipsoid (Oncley, 1941). The hydration factor f/f_e is represented by

$$f/f_e = \left(1 + \frac{w}{\rho\nu}\right)^{1/3}, \quad (10)$$

where w is the hydration defined as the number of grams water per gram of protein, ρ is the density of water, and ν is the partial specific volume of the macromolecule.

The frictional ratio for calmodulin (Eq. 8) in the absence and presence of calcium was calculated using experimental values of ν equal to 0.712 in the absence of calcium and 0.707 in the presence of calcium (Klee and Vanamon, 1982), and a molecular weight calculated on the basis of the amino acid sequence (16,695 g/mol). The hydration of CaM, w, was calculated using intrinsic hydration parameters for amino acids (Kuntz and Kauzmann, 1974), which are based on the assumption that one water molecule binds per amide group and one binds per side-chain polar group. In the absence of calcium w was calculated to be 0.459 for WT and 0.457 for all of the mutant proteins. However, in the presence of calcium, the hydration of five residues in each binding site is expected to decrease because of their chelation of calcium; thus those amino acids were treated as binding only 1 mole of water per residue, yielding a w of 0.386 for WT and 0.384 for the mutant proteins. The resulting difference in hydration upon calcium binding was 0.073 g H_2O/g protein for both wild-type and the mutant calmodulins. These values are higher than 0.25, a "typical" value of w that is often applied to globular proteins, but close to the "average" of 0.53 g H_2O/g protein as determined in a tabulation of 21 common proteins (Squire and Himmel, 1979). It should be noted that CaM is highly acidic (pI of less than 4).

Calculation of R_g

From the atomic coordinates of the 3cln structure of Ca_4^{2+}-CaM (Babu et al., 1988) and the models CaM10, R74A, and R90A (Fig. 3) derived from molecular dynamics simulations, the radius of gyration (R_g) was calculated using the FORTRAN program HYDRO (Garcia de la Torre and Bloomfield, 1981; Garcia de la Torre et al., 1994). Although this program was developed to allow calculations of hydrodynamic properties of macromolecules treated as aggregates of large beads or subdomains, it was applied to CaM and the models by including all nonhydrogen atoms and representing each as a bead with a radius of 1.53 Å (an average for C, N, and O).

RESULTS

A purpose of these studies was to test experimentally a theoretical proposal that Arg74 and Arg90 were residues critical for the formation of a compact, globular structure of Ca_4^{2+}-CaM (Pascual-Ahuir et al., 1991; Weinstein and Mehler, 1994) in which the N- and C-terminal domains are in a *cis* orientation and are closer than in the extended *trans* structure of 3cln (Babu et al., 1988). Gel permeation chromatography was used to compare the hydrodynamic behavior of wild-type CaM, R74A-CaM, R90A-CaM, and R90G-CaM under calcium-saturating and apo conditions at pH 7.4 and 5.6. The Stokes radii (R_s) for the three mutant proteins were compared to the wild type under these conditions. Analysis of shape changes in CaM due to mutation or induced by calcium binding was conducted, and comparisons of R_s values were made to those reported for compact globular proteins (Potschka, 1987; Pharmacia Biotech, 1996).

Stokes radius at pH 7.4

The Stokes radii of CaM, R74A-CaM, R90A-CaM, and R90G-CaM in the absence of calcium at pH 7.4 are shown in Fig. 5. The R_s of R74A-CaM was slightly greater than that of WT CaM; however, the difference was equivalent to the error in the determination. In contrast, the differences between the R90 mutants and WT appeared to be significant: R90A-CaM was 0.57 Å larger and R90G-CaM was 1.02 Å larger. When these proteins were saturated with calcium, only R74A-CaM was measurably (0.31 Å) larger than WT CaM.

For all of these proteins, calcium binding lowered the Stokes radius. The smallest net difference was seen for R74A-CaM (0.81 Å), a net change smaller than that of WT

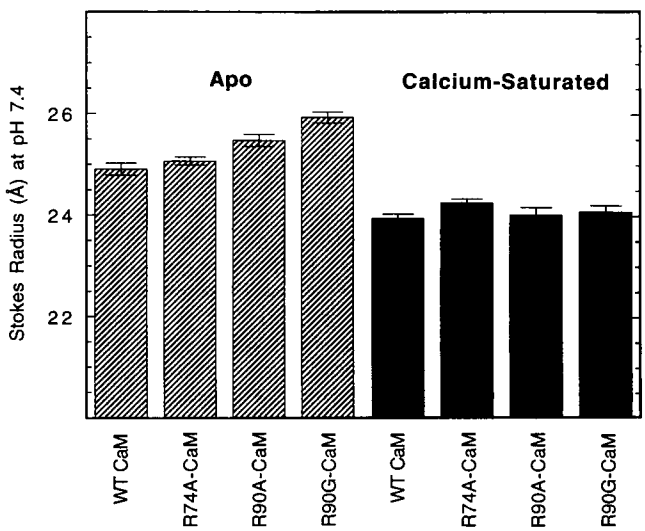

FIGURE 5 A comparison of calculated Stokes radii for apo (*hatched boxes*) and calcium-saturated (■) wild-type CaM, R74A-CaM, R90A-CaM, and R90G-CaM at pH 7.4, 23°C. All proteins were analyzed on a Pharmacia Superdex 75 column using a Basic Pharmacia FPLC system (Pharmacia Biotech). The elution profiles were monitored at 280 nm. Apo conditions were established using buffer C (50 mM HEPES, 91 mM KCl, 0.5 mM EGTA, 0.5 mM NTA (pCa 8.86 ± 0.18), pH 7.40 at 23°C); calcium-saturating conditions were established using buffer A (50 mM HEPES, 91 mM KCl, 0.5 mM EGTA, 0.5 mM NTA, 5.2 mM $CaCl_2$ (pCa 2.84 ± 0.01), pH 7.41 at 23°C). Stokes radii were calculated based on the elution profiles of standard proteins with known radii. All data represent an average of at least three determinations.

CaM (0.96 Å). The calcium-induced changes in R_s for both mutations at R90 were larger than that of WT; R90A-CaM decreased by 1.46 Å and R90G-CaM decreased by 1.84 Å upon calcium binding. Using the Stokes radii at pH 7.4, the value of f/f_o (Eq. 8) for apo WT CaM was calculated to be 1.244 and dropped slightly to 1.223 for Ca_4^{2+}-CaM.

Stokes radius at pH 5.6

Customarily, NMR and crystallographic studies of Ca_4^{2+}-CaM and apo-CaM have been conducted at pH lower than 7.4 (pH 5, Babu et al., 1988; pH 6, Ikura et al., 1991; Zhang et al., 1995; Kuboniwa et al., 1995; Finn et al., 1995). To explore the effect of pH on the shape of CaM, GPC studies of CaM were conducted in the absence and presence of saturating calcium at pH 5.6. The results from these studies of CaM, R74A-CaM, R90A-CaM, and R90G-CaM are illustrated in Fig. 6.

In the absence of calcium, the R_s values for R74A-CaM, R90A-CaM, and R90G-CaM at pH 5.6 were indistinguishable from wild-type values within the error of the experiment. In the presence of saturating calcium, R74A-CaM and wild-type were indistinguishable; the mutants at R90 were smaller than wild-type by 0.69 Å (R90A-CaM) and 0.30 Å (R90G-CaM). For both levels of calcium, the R_s values at pH 5.6 were smaller than those measured for the corresponding protein at pH 7.4. Based on the Stokes radii for WT CaM at pH 5.6, the value of f/f_o (Eq. 8) for apo WT CaM was 1.196 and decreased slightly to 1.188 for Ca_4^{2+}-CaM. These values were slightly smaller than the corresponding values at pH 7.4.

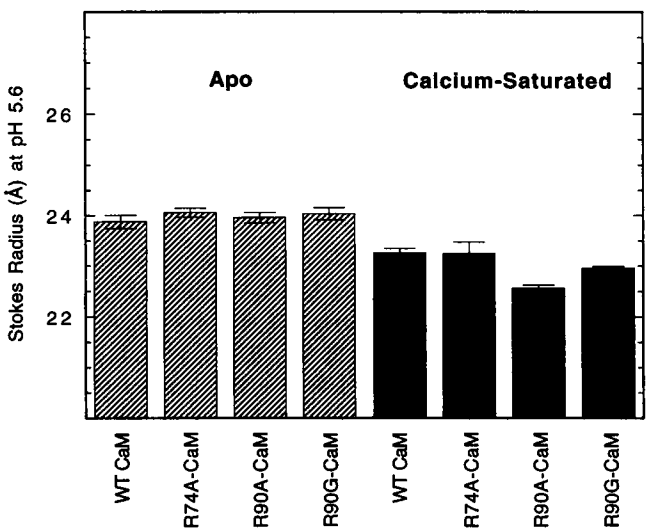

FIGURE 6 A comparison of calculated Stokes radii for apo (*hatched boxes*) and calcium-saturated (■) wild-type CaM, R74A-CaM, R90A-CaM, and R90G-CaM at pH 5.6, 23°C. All proteins were run on a Pharmacia Superdex 75 column using a Basic Pharmacia FPLC system (Pharmacia Biotech). The elution profiles were monitored at 280 nm. Apo conditions were established using buffer D (50 mM PIPES, 89 mM KCl, 0.5 mM EGTA, 0.5 mM NTA (pCa 6.64 ± 0.63), pH 5.61 at 23°C); calcium-saturating conditions were established using buffer B (50 mM PIPES, 89 mM KCl, 0.5 mM EGTA, 0.5 mM NTA, 5.2 mM $CaCl_2$ (pCa 2.27 ± 0.01), pH 5.60 at 23°C). Stokes radii were calculated as described for studies at pH 7.4. All data represent an average of at least three determinations.

State of association

The determination of a Stokes radius from small-zone analytical gel permeation chromatography studies assumes that the single peak observed represents the elution behavior of a monomer species of the protein. Although x-ray scattering studies of CaM at pH 5.5 and 6.0 in the absence and presence of calcium indicated that CaM exists as a monomer (Heidorn and Trewhella, 1988; Yoshino et al., 1993), one study reported signs of CaM aggregation at pH 5.5 (Heidorn and Trewhella, 1988). To ensure that CaM existed as a monomer under all of the conditions used in these studies, concentration-dependent analyses were conducted at pH 7.4 and 5.6. The value of R_s determined at pH 7.4 for 300 μM Ca_4^{2+}-CaM was indistinguishable from that determined at 93 μM Ca_4^{2+}-CaM and is in agreement with other reports (Seaton et al., 1985; Heidorn and Trewhella, 1988). At pH 5.6 the values of R_s for 20 μM and 40 μM Ca_4^{2+}-CaM were also indistinguishable and only slightly smaller (0.15 Å) than that observed for 93 μM Ca_4^{2+}-CaM. These results indicated that Ca_4^{2+}-CaM appeared to be monomeric at the concentrations and solution conditions used in these studies.

Calculation of R_g and comparison to R_s of standards

Weinstein and co-workers (Weinstein and Mehler, 1994; Pascual-Ahuir et al., 1991) calculated the radius of gyration (R_g) of the CaM10 model to be 17 Å (Pascual-Ahuir et al., 1991). Calculations of R_g from the coordinates of 3cln and the molecular dynamics models CaM10, R74A, and R90A (Fig. 3) are listed in Table 1 for comparison. The value of R_g calculated for CaM10 (16.99 Å) was identical to the value reported previously and was smaller than the R_g of the R74A model (24.02 Å) and the R90A model (24.32 Å), as predicted (Pascual-Ahuir et al., 1991). There is no atomic model for the structure of the R90G-CaM mutant, and therefore R_g could not be calculated.

Also shown in Table 1 are values of R_s, R_g, and molecular weight (Potschka, 1987; Pharmacia Biotech, 1996) for common proteins that are regarded as having compact structures. Comparison of these values indicated that in all cases the experimentally determined Stokes radius is larger than the calculated value of R_g. This difference was also found in cases where R_s could be compared to experimentally determined values of R_g.

DISCUSSION

The studies presented demonstrate the use of small-zone analytical gel permeation chromatography (GPC) to resolve

calcium-dependent conformational changes in wild-type and mutant CaM. This approach has been used to study the hydrodynamic properties of many proteins (Ackers, 1964, 1967, 1970; Andrews, 1964, 1965, 1970; Laurent and Killander, 1964; Squire, 1964; Henn and Ackers, 1969; Warshaw et al., 1971; Tanford et al., 1974; Horiike et al., 1983; Potschka, 1987; Le Maire et al., 1989). Studies by Ackers and co-workers (Warshaw and Ackers, 1971) showed that the inherent precision of molecular radius determinations of globular proteins by gel partitioning methods is ±0.2 Å, a value that is in good agreement with those reported here. On this basis, small differences in Stokes radii measurements allow us to compare the behavior of mutants to that of wild-type CaM and to explore the effects of changing solution conditions.

The size and shape of CaM are characterized by plasticity that is essential to its function as a calcium-sensitive activator. A crystallographic structure for Ca_4^{2+}-CaM (Babu et al., 1988) indicated that CaM had the dimensions 65 × 30 × 30 Å (Clore and Gronenborn, 1994); however, small-angle (Heidorn and Trewhella, 1988, 1990) and solution x-ray scattering (Yoshino et al., 1989, 1993) studies suggest that the average separation of the domains of Ca_4^{2+}-CaM is smaller than that observed in 3cln. A fluorescence anisotropy study of wheat germ CaM with Cys27 cross-linked to Tyr139 (Small and Anderson, 1988) indicated that variation in determination of the solution structure for Ca_4^{2+}-CaM may be due to hydration. It demonstrated that an ~3 Å decrease in the overall dimension of Ca_4^{2+}-CaM was possible when the value assumed for the hydration increased from 0.2 to 0.4 g H_2O/g Ca_4^{2+}-CaM. Small and Anderson also reported that the increase in volume associated with 0.4 g H_2O/g Ca_4^{2+}-CaM hydration would require the two domains to nearly touch (Small and Anderson, 1988). Several lines of evidence, including absorption spectroscopy studies (Yazawa et al., 1990) and quantitative proteolytic footprinting studies (Pedigo and Shea, 1995; Shea et al., 1996), suggest that the domains are not rigidly separated in CaM; time-resolved fluorescence anisotropy studies indicate that Ca_4^{2+}-CaM may exist in solution as a compact globular protein (Bayley et al., 1988).

These inconsistencies prompted a series of molecular dynamics studies (Pascual-Ahuir et al., 1991; Mehler et al., 1991; Weinstein and Mehler, 1994) designed to model the energy-minimized structure for Ca_4^{2+}-CaM. Simulations predicted a structural model (CaM2 or CaM10) that was smaller than the 3cln crystal structure (Babu et al., 1988). In the simulations, a ratcheting motion of arginine residues bent the flexible tether region of Ca_4^{2+}-CaM to bring the domains closer to each other. The domains of CaM2 and CaM10 adopted a *cis* orientation (Pascual-Ahuir et al., 1991; Mehler et al., 1991; Weinstein and Mehler, 1994) rather than the *trans* orientation observed in the 3cln crystal structure. The radius of gyration (R_g) for the model CaM10 (16.99 Å) and 3cln (21.91 Å), calculated using HYDRO, indicated that CaM10 was 4.92 Å smaller than 3cln. This predicted difference in molecular size was expected to be directly detectable by experimental studies and prompted the series of gel permeation chromatography studies presented here to test the model of compaction.

Molecular size

The Stokes radius of Ca_4^{2+}-CaM at pH 7.4 was determined to be 23.95 Å and is in good agreement with one reported previously (Dedman et al., 1977). In comparison to calibration proteins of similar molecular weight, the experimentally determined R_s of CaM (in both the presence and absence of calcium) is higher than expected. This comparison holds when CaM is compared to another protein organized as two domains separated by a linker: the R_s (24.91 Å) of apo-CaM (148 residues) is larger than the R_s (23 Å; Burz et al., 1994) of a monomer of lambda cI repressor (236 residues).

In Table 1 a comparison of the Stokes radii reported for globular proteins of molecular weight similar to that of CaM (Potschka, 1987; Pharmacia Biotech, 1996), with their R_g values calculated with HYDRO, illustrated that for these globular proteins, R_s was approximately 2–4 Å larger than the radius of gyration. This difference in R_s is in good agreement with the difference between R_g values obtained for CaM using SAXS (Seaton et al., 1985; Heidorn and Trewhella, 1988, 1990; Kataoka et al., 1989, 1991a,b; Matsushima et al., 1989) and the R_s obtained using GPC for CaM in this study. Therefore, the radius of gyration for Ca_4^{2+}-CaM may be estimated as 20–22 Å, and comparison to the value of R_g predicted based on molecular dynamics (17 Å) would suggest that the average size of the structure of Ca_4^{2+}-CaM is more similar to the 3cln crystallographic structure than to CaM10.

Pair distribution function

Calcium-induced conformational changes in CaM have been analyzed using small-angle x-ray scattering (Seaton et al., 1985; Heidorn and Trewhella, 1988; Kataoka et al., 1989, 1991a,b; Matsushima et al., 1989) and solution x-ray scattering (Yoshino et al., 1989, 1993). These studies all indicated a small increase in the radius of gyration (R_g) of CaM upon binding calcium; however, the magnitude of this increase varied from 0.1 Å (Heidorn and Trewhella, 1988) to 2.5 Å (Yoshino et al., 1993) and depended on whether the data were analyzed using the Guinier or Moore approach. The discrepancy between these two approaches could be rationalized by assuming an equilibrium among structures of CaM whose domains were in various states of reorientation and compaction (Mehler et al., 1991). One way to treat this is to consider the measured properties as an average of the behavior of the limiting cases.

Weinstein and Mehler (Mehler et al., 1991) derived a pair distribution function for the simulated model CaM2 and compared it to the pair distribution function obtained in small-angle x-ray scattering studies (Heidorn and Tre

whella, 1988; Kataoka et al., 1989, 1991a; Matsushima et al., 1989) in an attempt to estimate the fraction (α) of the total population represented by the extended structure. Making the assumption that CaM in solution is an equilibrium mixture of two structures similar to CAM2 and 3cln (x-ray), this fraction was expressed as

$$\alpha = [R_g^2(\alpha) - R_g^2(\text{CaM2})]/[R_g^2(\text{x-ray}) - R_g^2(\text{CaM2})], \quad (11)$$

where the R_g values were estimated or calculated as follows. The value of 21.5 Å for $R_g(\alpha)$ was determined for Ca_4^{2+}-CaM in solution using SAXS (Matsushima et al., 1989), the value of 17.8 Å used for R_g(CaM2) was the SAXS value reported for a CaM:mastoparan complex, and the value of 22.8 Å used for R_g(x-ray) was one calculated using a dumbbell model in which two ellipsoids (20.5 × 13 Å) represented the domains of CaM and a single ellipsoid (30 × 7 Å) represented the interconnecting helix (Heidorn and Trewhella, 1988). The resulting value of α was 71%, suggesting that a compact structure like CaM2 could represent almost 30% of the total population of Ca_4^{2+}-CaM species in solution.

However, the value of α is extremely sensitive to small differences in the values of R_g. Using an R_g(CaM2) of 17.2 Å and R_g(x-ray-3cln) of 22.0 Å as calculated by CHARMM (see table 2 in Mehler et al., 1991), the value of α increases to 88%, implying that a compact structure exists at a level of only 12%. If R_g is calculated using HYDRO, R_g(CaM10) is 16.99 Å and R_g(x-ray) is 21.91 Å; the value of α changes to 91%. These two examples illustrate the sensitivity of the calculation to the precise R_g values and demonstrate that experimental error could cause large variability in the predicted fractional population of a compact structure such as CaM2 or CaM10 in an equilibrium distribution in solution. If an extended 3cln-like structure represents at least 90% of the total, it is possible that small-zone analytical GPC studies would not detect the presence of a compact species contributing only 10%, particularly if there were a dynamic equilibrium between these as expected for CaM.

Molecular shape

Previous studies (cf. Squire and Himmel, 1979) have shown that the frictional-based Stokes equation provides a good estimate of the behavior of proteins with molecular weights similar to that of CaM. The frictional ratios f/f_o for Ca_4^{2+}-CaM were calculated and found to lie within a range delimited by the proteins in Table 1; however, this does not imply that CaM behaves as a globular protein under the conditions used in this study. (The reported frictional ratio for bovine serum albumin (BSA) is 1.308, yet the dimensions for this protein (140 × 40 × 40 Å) derived from its crystal structure are hardly "spherical" (Squire and Himmel, 1979).) Because the experimentally determined R_s of CaM is much greater than that expected for a protein of its molecular weight, the *a/b* ratio for an equivalent prolate ellipsoid is quite skewed (values ranging from 4 to 5). Thus these data support the contention that CaM may behave on average more as a dumbbell or perhaps an hourglass (as suggested by spectroscopic data; Small and Anderson, 1988; Bayley et al., 1988; Yao et al., 1994; Tjandra et al., 1995). Further interpretation of the frictional ratio awaits an experimental determination of hydration properties that are complex (Kita et al., 1994), especially for this highly charged protein, which exposes a large hydrophobic cleft upon binding calcium (LaPorte et al., 1980).

Calcium-induced structural changes

Structural, chemical, and spectroscopic studies over the last 20 years have indicated that CaM changes size and shape upon calcium binding. Studies using NMR (Seamon, 1980; Ikura et al., 1983, 1984, 1985; Klevit et al., 1984; Hoffman and Klevit, 1991), dynamic fluorescence anisotropy (Small and Anderson, 1988; Török et al., 1992), lifetime-resolved fluorescence resonance energy transfer (Yao et al., 1994), and small-angle and solution x-ray scattering (Seaton et al., 1985; Heidorn and Trewhella, 1988, 1990; Kataoka et al., 1989, 1991a,b; Matsushima et al., 1989; Yoshino et al., 1989, 1993), and chemical and proteolytic cleavage (Pedigo and Shea, 1995; Shea et al., 1996) have shown that apo-CaM is flexible relative to most globular proteins and becomes more rigid upon binding calcium. These studies are supported by an increase in solvent accessibility (Yao et al., 1994) and the volume of CaM (Kupke, 1986; Kupke and Shank, 1989; Török et al., 1992) upon binding calcium. Small-angle x-ray scattering studies have shown that the radius of gyration increased by a range of 0.1 Å (Heidorn and Trewhella, 1988) to 2.5 Å (Yoshino et al., 1993) upon binding calcium, and the maximum dimension between two atoms (d_{max}) in CaM increased by a range of 4 Å (Heidorn and Trewhella, 1988; Seaton et al., 1985) to 5 Å (Kataoka et al., 1989, 1991a). Recent NMR structures provide quantitative insight into the calcium-induced reorientation of the helices within each EF-hand motif as they go from being almost parallel in the absence of calcium to almost perpendicular in the presence of calcium (Ikura et al., 1991; Kuboniwa et al., 1995; Zhang et al., 1995; Finn et al., 1995). These studies all suggest that each domain of Ca_4^{2+}-CaM in solution has a greater surface area, less flexibility, and a greater average separation relative to apo-CaM.

In the gel permeation chromatography studies presented here, the Stokes radius of hydrated CaM decreased by 0.96 Å upon addition of calcium. Other reports of the Stokes radius for Ca_4^{2+}-CaM are in agreement with those reported here (Dedman et al., 1977; Crouch and Klee, 1980), and one showed a 0.5 Å decrease upon binding calcium (Crouch et al., 1980). In contrast, SAXS studies performed in several laboratories consistently demonstrate a small but reproducible increase in R_g values for CaM upon saturation by calcium (Seaton et al., 1985; Heidorn and Trewhella, 1988, 1990; Kataoka et al., 1989, 1991a,b; Matsushima et al., 1989; Yoshino et al., 1989, 1993). Although the direction of

the calcium-induced change in R_s is opposite to the change in R_g observed in SAXS studies, numerous repetitions of the GPC studies under various conditions (e.g., variation of temperature from 4°C to 23°C, different instrumentation (fast protein liquid chromatography (FPLC) and HPLC), protein stock, and buffer composition) yielded consistent results. The precision in R_s reported in Table 2 (0.03–0.23 Å) reflects the precision attainable in the elution volumes (0.01–0.05 ml) and the reproducibility of the column. Equivalent results have been obtained by five individuals in this laboratory. In addition, gel permeation studies of recombinant *Paramecium* CaM (wild type and 12 mutants) all showed a decrease in R_s upon saturation by calcium (Harmon and Shea, 1995; Chen and Shea, data not shown). This large body of evidence supports the validity of the small differences reported here. Although the discrepancy between the GPC and SAXS results is not understood, it demonstrates that these techniques measure subtly different properties of CaM in solution.

Separable contributions of domains

The shape of each domain is determined by the relative orientations of the two component EF-hands: the four helices and their linker sequences. For reference, Fig. 2 shows the third EF-hand of Ca_4^{2+}-CaM as observed in the x-ray crystallographic structure 3cln.pdb (Babu et al., 1988). Structures of Ca_4^{2+}-CaM determined by x-ray diffraction (XRD) (Babu et al., 1985, 1988; Taylor et al., 1991; Chattopadhyaya et al., 1992) and NMR (Ikura et al., 1991; Barbato et al., 1992) have shown that both domains are globular, with approximate dimensions of 20 × 20 × 25 Å (Babu et al., 1985). In Ca_4^{2+}-CaM the helices within a single EF-hand are almost perpendicular (calculated interhelical angles range from 84 Å between the C/D helix pair in the N-terminal domain to 105 Å between the E/F helix pair in the C-terminal domain; Kuboniwa et al., 1995). Interhelical distances (defined as the distance between the centers of the axes of the EF-hand helices; Zhang et al., 1995) range from 14.4 Å (between the G and H helices flanking site IV) to 18.5 Å (between the A and B helices flanking site I) (Zhang et al., 1995; Finn et al., 1995).

The calcium-induced structural changes in CaM currently cannot be addressed by XRD methods because there is no crystallographic determination of a structure of apo-CaM. Early 1-D proton NMR analysis of stoichiometric calcium binding studies (Seamon, 1980; Ikura et al., 1983, 1984; Klevit et al., 1984; Aulabaugh et al., 1984; Urbauer et al., 1995) indicated that domains changed sequentially with the C-terminal domain calcium-binding sites having higher affinity for calcium than the N-terminal domain sites; however, the chemical shifts of a few N-terminal domain residues changed over the range of zero to two calcium ions bound per CaM, suggesting domain interactions.

A detailed structural comparison of the effect of calcium on whole CaM has been made possible by recent NMR determinations of apo-CaM structures (Zhang et al., 1995; Kuboniwa et al., 1995). Comparison of these with a crystallographic study of Ca_4^{2+}-CaM (Babu et al., 1988) indicated that there is no major change in the secondary structure of CaM. However, the helices within each EF-hand change from an almost antiparallel orientation to an almost perpendicular orientation upon binding calcium. The increase in interhelical distance upon binding calcium ranged from 2.1 Å (for the G-H helix pair) to 6.2 Å (for the A-B helix pair). Superposition of the NMR models for apo-CaM indicated that the relative orientation of the two domains was not constrained (the family of structures were manifest as a "mushroom") (Zhang et al., 1995).

NMR studies of the isolated C-terminal domain of CaM (residues 76–148) indicated that the secondary structure of the domain was conserved upon binding calcium but rearranged to give a more open structure with a 3.6-Å increase in the interhelical distance (Finn et al., 1995). Calculation of the radius of gyration using HYDRO (Garcia de la Torre et al., 1994; Garcia de la Torre and Bloomfield, 1981) for the structural models 1 and 20 of the C-terminal domain in apo (1cmf.pdb) and calcium-saturated forms (1cmg.pdb; Finn et al., 1995) indicated that the radius of gyration increased by ~1.5 Å upon binding calcium. These differences are possibly due to the significant mobility observed for the first six residues, the linker and the two calcium-binding loops of the C-terminal domain.

Calcium-induced changes in the size of CaM reflect changes intrinsic to each domain and to the relative disposition of the domains; the difference in Stokes radius between apo- and Ca_4^{2+}-CaM may be expressed as

$$\Delta R_s = f(\Delta N) + f(\Delta C) + f(\Delta(N \leftrightarrow C)), \qquad (12)$$

where $f(\Delta N)$ is a function of calcium-induced change intrinsic to the N-terminal domain, $f(\Delta N)$ is the corresponding term for the C-terminal domain, and $f(\Delta(N \leftrightarrow C))$ represents changes in the orientation of the domains upon binding calcium. To evaluate each of these contributions, preliminary GPC studies of recombinant forms of the N-terminal domain (residues 1–75) and C-terminal domain (residues 76–148) of CaM were conducted in the absence and presence of calcium at pH 7.4, 23°C. These indicated that 1) the overall size of each domain was larger than predicted by comparison with calibration proteins or on the basis of calculations of R_g from coordinates of CaM structures and that 2) the Stokes radius decreased slightly upon binding

TABLE 2 Calcium and pH dependence of Stokes radius of calmodulin

	R_s (Å) at pH 7.4		R_s (Å) at pH 5.6	
	Apo-CaM	Ca_4^{2+}-CaM	Apo-CaM	Ca_4^{2+}-CaM
WT CaM	24.91 ± 0.12	23.95 ± 0.09	23.88 ± 0.13	23.26 ± 0.09
R74A-CaM	25.07 ± 0.08	24.26 ± 0.08	24.06 ± 0.09	23.25 ± 0.23
R90A-CaM	25.48 ± 0.12	24.02 ± 0.15	23.96 ± 0.10	22.57 ± 0.06
R90G-CaM	25.93 ± 0.11	24.09 ± 0.13	24.04 ± 0.12	22.96 ± 0.03

calcium (Sorensen and Shea, data not shown). However, further analysis will be required to assess the contribution of the orientation of the two domains to ΔR_s.

Effects of pH

Gel permeation studies of Ca_4^{2+}-CaM were conducted at pH 5.6 to allow direct comparisons of the Stokes radius for Ca_4^{2+}-CaM to 3cln, a crystal structure determined at pH 5 (Babu et al., 1988). The measured Stokes radius for Ca_4^{2+}-CaM at pH 5.6 was 23.26 ± 0.09 Å. The overall length of CaM in 3cln was reported to be 65 Å, with each domain being 20 × 20 × 25 Å (Cook and Sack, 1983; Babu et al., 1985, 1988); analysis of 3cln using HYDRO indicated that its radius of gyration would be 21.91 Å. For globular proteins of molecular weight similar to that of CaM (Potschka, 1987; Pharmacia Biotech, 1996), the experimentally determined R_s was consistently 2–4 Å larger than the R_g value calculated with HYDRO. This offset is in good agreement with the differences between the R_g obtained for CaM using SAXS (Seaton et al., 1985; Heidorn and Trewhella, 1988, 1990; Kataoka et al., 1989, 1991a,b; Matsushima et al., 1989) and the R_s obtained using GPC for CaM in this study. Therefore, a R_s of 23.26 ± 0.09 Å is roughly equivalent to the R_g determined for 3cln. Comparison of the helical content of Ca_4^{2+}-CaM in solution at pH 5 measured by far-UV CD (Bayley et al., 1988; Bayley and Martin, 1992; Török et al., 1992) to that observed in 3cln showed that 3cln had a higher degree of α-helical content than in solution, which was attributed to the helicogenic compounds added to promote crystallization (Bayley and Martin, 1992).

The calcium-induced changes in R_s for CaM at pH 5.6 are illustrated in Fig. 6. The results indicated that the Stokes radius decreased by a slightly smaller amount (0.62 Å) upon addition of calcium than the 0.96 Å decrease observed at pH 7.4 (Table 2). Comparing the Stokes radius for Ca_4^{2+}-CaM or apo-CaM determined at pH 5.6 to the corresponding values determined at pH 7.4 indicated that under both conditions CaM increased in size as the pH was increased. Far-UV CD studies would suggest that this increase is not due to changes in helical content (Török et al., 1992; Bayley and Martin, 1992). Fluorescence energy transfer (Wang, 1989) showed a reduced quenching of the emission from Tb^{3+} in the four binding sites by a chromophore attached to Cys27; this could indicate elongation of Ca_4^{2+}-CaM at pH 5 relative to pH 7. However, it could be due to a *cis/trans* reorientation of the domains such that Cys27 is more distant from the terbium ions under more acidic conditions.

Gel permeation chromatography studies of CaM mutants

A goal of this study was to test experimentally a theoretical proposal that Arg74 and Arg90 were critical for the formation of a compact, globular structure (Pascual-Ahuir et al., 1991; Weinstein and Mehler, 1994) of Ca_4^{2+}-CaM. The predictions for the existence of this structure and the experimental analysis by gel permeation chromatography at pH 7.4 and 5.6 have been discussed. The proposal that Arg74 and Arg90 are important for the formation of the structure of Ca_4^{2+}-CaM can be evaluated regardless of the atomic details of the resulting structures. In addition to the R74A-CaM and R90A-CaM mutant proteins, an Arg90-to-glycine mutation (R90G-CaM) was also made to introduce a possible disruption of the helix leading into site III and thereby probe the importance of this helix in determining the structure of CaM in the absence or presence of calcium.

The modeled structures of R74A-CaM (R74A model) and R90A-CaM (R90A model) are depicted in Fig. 3. The orientation of the domains in the R74A model and the R90A model are *cis*, as was observed for CaM10 and contrary to the *trans* orientation observed in 3cln (Babu et al., 1988). The dihedral angle (see Eq. 1) reported for CaM10 was −72°, and that reported for the R74A model (−77°) was similar to CaM10 but larger than the −43° reported for the R90A model (Weinstein and Mehler, 1994). Molecular dynamics predicted that the mutation of Arg74 or Arg90 would result in conformations more extended than that of 3cln (Pascual-Ahuir et al., 1991). As indicated in Table 1, an analysis of the radius of gyration for the R74A model and the R90A model using HYDRO showed that the R74A model was 7.03 Å larger than CaM10 and 2.11 Å larger than 3cln; the R90A model was 7.33 Å larger than CaM10 and 2.41 Å larger than 3cln. Despite the larger dimension of the R90A model, the largest deviation from CaM10 was predicted for the R74A model because in the molecular dynamics simulations this residue was always involved in a hydrogen bonding interaction with at least two residues (Weinstein and Mehler, 1994).

Fig. 5 illustrates the results obtained from the study of R74A-CaM, R90A-CaM, and R90G-CaM relative to wild-type CaM in the absence and presence of calcium at pH 7.4, and Fig. 6 illustrates the corresponding studies performed at pH 5.6. At pH 7.4 the only difference in R_s relative to wild type in the presence of saturating calcium was observed for R74A-CaM (0.31 Å). This is in agreement with that predicted from molecular dynamics; however, the magnitude of the increase in R_s is significantly smaller than the predicted increase in R_g (7.03 Å relative to CaM10 and 2.11 Å relative to 3cln). The more significant changes in R_s for the mutants relative to wild type were seen in the absence of calcium at pH 7.4, where R90A-CaM was 0.57 Å larger than wild-type CaM and R90G-CaM was 1.02 Å larger than wild type. Thus the greatest difference in Stokes radius relative to wild type under all conditions used in this study was observed at pH 7.4 in the absence of calcium, when the helix leading into site III was disrupted by introducing a glycine in place of an arginine.

These results suggest that at pH 7.4, Arg90 may play a role in the degree of compaction of apo-CaM; however, they do not support any role in the presence of calcium. At pH 5.6, the only differences observed in R_s relative to wild-type

CaM was in the presence of saturating calcium, and the direction of the difference was opposite that observed at pH 7.4, where the mutants were larger than wild type. At pH 5.6, the Stokes radius for R74A-CaM and wild-type CaM were indistinguishable, the R_s for R90A-CaM was 0.69 Å smaller than wild-type CaM, and R90G-CaM was 0.30 Å smaller than wild-type CaM. The results presented here suggest that the average size of Ca_4^{2+}-CaM in solution is more similar to 3cln than to the compact structure of CAM10 predicted by molecular dynamics (Mehler et al., 1991; Pascual-Ahuir et al., 1991). Although no direct evidence was provided for the existence of an abundant compact structure for Ca_4^{2+}-CaM, the fractional abundance of such a species may be too small to be detected by gel permeation chromatography.

Other properties of these mutants are similar to those of wild-type CaM. Preliminary quantitative thrombin footprinting studies of R74A-CaM, R90A-CaM, and R90G-CaM at pH 7.4 (data not shown) showed a pattern of calcium-dependent cleavage at Arg37 and Arg106 similar to that of wild-type CaM (Shea et al., 1996). These data suggested that calcium binding energetics are similar and that whatever structural changes in Ca_4^{2+}-CaM are induced by mutation at Arg74 or Arg90, they do not destroy the domain-domain interactions present in wild-type CaM. Preliminary studies of chemically induced unfolding of these mutants in the absence of calcium at pH 7.4 indicated that their stability was indistinguishable from that of wild-type CaM (data not shown) and suggest that minimal secondary structural rearrangements were induced by these mutations for the apo form. Additional studies using circular dichroism, UV absorption spectroscopy, and fluorescence spectroscopy are being conducted to explore further the calcium-induced changes in the structural properties of CaM induced by these mutations.

The differences between Stokes radius and radius of gyration that are indicated by this study suggest that there are compensating elements of conformational change and differential hydration that determine the calcium-induced changes in hydrodynamic properties of calmodulin. These differences underscore the need to understand the properties of isolated domains further and to use multiple techniqes (structural and hydrodynamic) to assess the properties of the holo protein.

We dedicate this manuscript to Serge Timasheff, whose leadership in the study of macromolecules and their interactions with each other and solvents has influenced many and set a standard to which we aspire. We would like to thank H. Weinstein for sharing the coordinates of the structures of CaM10, R74A, and R90A models predicted by molecular dynamics; R. Mauer and P. Howard for the overexpression vector used for WT calmodulin; D. Tinker and C. R. Kephart for the preparation of R90A-CaM; S. Harmon for the preparation of R74A-CaM; A. Bergold of the University of Iowa College of Medicine Protein Structure Facility for the amino acid analysis; D. Moser of the DNA Facility of the Diabetes and Endocrinology Research Center, University of Iowa College of Medicine for DNA sequencing; and the reviewers for helpful suggestions.

These studies were supported by grants to MAS from the American Heart Association (910148980), a National Science Foundation Presidential Young Investigator Award (NSF DMB 9057157), and the National Institutes of Health Diabetes and Endocrinology Research Center (DK 25295).

REFERENCES

Abola, E. E., F. C. Bernstein, S. H. Bryant, T. F. Koetzleand, and J. Weng. 1987. Protein Data Bank. *In* Crystallographic Databases—Information Content, Software Systems, Scientific Applications. F. H. Allen, G. Bergerhoff and R. Sievers, editors. Data Commission of the International Union of Crystallography, Bonn/Cambridge/Chester. 107–132.

Ackers, G. K. 1964. Molecular exclusion and restricted diffusion processes in molecular-sieve chromatography. *Biochemistry.* 3:723–730.

Ackers, G. K. 1967. A new calibration procedure for gel filtration columns. *J. Biol. Chem.* 242:3237–3238.

Ackers, G. K. 1970. Analytical gel chromatography of proteins. *Adv. Protein Chem.* 24:343–446.

Ackers, G. K., and T. E. Thompson. 1965. Determination of stoichiometry and equilibrium constants for reversibly associating systems by molecular sieve chromatography. *Proc. Natl. Acad. Sci. USA.* 53:342–349.

Andrews, P. 1964. Estimation of the molecular weights of proteins by Sephadex gel-filtration. *Biochem. J.* 91:222–233.

Andrews, P. 1965. The gel-filtration behaviour of proteins related to their molecular weights over a wide range. *Biochem. J.* 96:595–606.

Andrews, P. 1970. Estimation of molecular size and molecular weights of biological compounds by gel filtration. *In* Methods of Biochemical Analysis. D. Glick, editor. John Wiley and Sons, New York. 1–53.

Aulabaugh, A., W. P. Niemczura, and W. A. Gibbons. 1984. High field proton NMR studies of tryptic fragments of calmodulin: a comparison with the native protein. *Biochem. Biophys. Res. Commun.* 118:225–232.

Babu, Y. S., C. E. Bugg, and W. J. Cook. 1988. Structure of calmodulin refined at 2.2 Å resolution. *J. Mol. Biol.* 204:191–204.

Babu, Y. S., J. S. Sack, T. J. Greenhough, C. E. Bugg, A. R. Means, and W. J. Cook. 1985. Three-dimensional structure of calmodulin. *Nature.* 315:37–41.

Barbato, G., M. Ikura, L. E. Kay, R. W. Pastor, and A. Bax. 1992. Backbone dynamics of calmodulin studied by ^{15}N relaxation using inverse detected two-dimensional NMR spectroscopy: the central helix is flexible. *Biochemistry.* 31:5269–5278.

Bayley, P. M., and S. R. Martin. 1992. The α-helical content of calmodulin is increased by solution conditions favouring protein crystallisation. *Biochim. Biophys. Acta.* 1160:16–21.

Bayley, P., S. Martin, and G. Jones. 1988. The conformation of calmodulin: a substantial environmentally sensitive helical transition in Ca4-calmodulin with potential mechanistic function. *FEBS Lett.* 238: 61–66.

Bernstein, F. C., T. F. Koetzle, G. J. B. Williams, E. F. Meyer, Jr., M. D. Brice, J. R. Rodgers, O. Kennard, T. Shimanouchi, and M. Tasumi. 1977. The Protein Data Bank: a computer-based archival file for macromolecular structures. *J. Mol. Biol.* 112:535–542.

Burz, D. S., D. Beckett, N. Benson, and G. K. Ackers. 1994. Self-assembly of bacteriophage λ cI repressor: effects of single-site mutations on the monomer-dimer equilibrium. *Biochemistry.* 33:8399–8405.

Chattopadhyaya, R., W. E. Meador, A. R. Means, and F. A. Quiocho. 1992. Calmodulin structure refined at 1.7 Å resolution. *J. Mol. Biol.* 228: 1177–1192.

Clore, G. M., and A. M. Gronenborn. 1994. Structures of larger proteins, protein-ligand and protein-DNA complexes by multidimensional heteronuclear NMR. *Protein Sci.* 3:372–390.

Cook, W. J., and J. S. Sack. 1983. Preparation of calmodulin crystals. *Methods Enzymol.* 102:143–147.

Cook, W. J., L. J. Walter, and M. R. Walter. 1994. Drug binding by calmodulin: crystal structure of a calmodulin-trifluoperazine complex. *Biochemistry.* 33:15259–15265.

Cox, J. A. 1988. Interactive properties of calmodulin. *Biochem. J.* 249: 621–629.

Crivici, A., and M. Ikura. 1995. Molecular and structural basis of target recognition by calmodulin. *Annu. Rev. Biophys. Biomol. Struct.* 24: 85–116.

Crouch, T. H., and C. B. Klee. 1980. Positive cooperative binding of calcium to bovine brain calmodulin. *Biochemistry.* 19:3692–3698.

Davis, T. N., M. S. Urdea, F. R. Masiarz, and J. Thorner. 1986. Isolation of the yeast calmodulin gene: calmodulin is an essential protein. *Cell.* 47:423–431.

Dedman, J. R., J. D. Potter, R. L. Jackson, J. D. Johnson, and A. Means. 1977. Physicochemical properties of rat testis Ca^{2+}-dependent regulator protein of cyclic nucleotide phosphodiesterase relationship of Ca^{2+}-binding, conformational changes, and phosphodiesterase activity. *J. Biol. Chem.* 252:8415–8422.

Finn, B. E., J. Evenäs, T. Drakenberg, J. P. Waltho, E. Thulin, and S. Forsén. 1995. Calcium-induced structural changes and domain autonomy in calmodulin. *Nature Struct. Biol.* 2:777–783.

Garcia de la Torre, J., and V. A. Bloomfield. 1981. Hydrodynamic properties of complex, rigid, biological macromolecules: theory and applications. *Q. Rev. Biophys.* 14:81–139.

Garcia de la Torre, J., S. Navarro, M. C. Lopez Martinez, F. G. Diaz, and J. J. Lopez Cascales. 1994. HYDRO: a computer program for the prediction of hydrodynamic properties of macromolecules. *Biophys. J.* 67:530–531.

George, S. E., Z. Su, D. Fan, and A. R. Means. 1993. Calmodulin-cardiac troponin C chimeras: effects of domain exchange on calcium binding and enzyme activation. *J. Biol. Chem.* 265:2513–25220.

Harmon, S. D., and M. A. Shea. 1995. Allosteric disruption of paramecium calmodulin. *Biophys. J.* 68:A140.

Heidorn, D. B., and J. Trewhella. 1988. Comparison of the crystal and solution structures of calmodulin and troponin C. *Biochemistry.* 27: 909–915.

Heidorn, D. B., and J. Trewhella. 1990. Low resolution studies of proteins in solution: calmodulin. *Comments Mol. Cell Biophys.* 6:329–359.

Henn, S. W., and G. K. Ackers. 1969. Molecular sieve studies of interacting protein systems. V. Association of subunits of D-amino acid oxidase apoenzyme. *Biochemistry.* 8:3829–3838.

Hoffman, R. C., and R. E. Klevit. 1991. Structural analysis of the amino-terminal domain of apo-calmodulin by ^{1}H-homonuclear 2D-NMR. *In* Techniques in Protein Chemistry II. J. Villafranca, editor. Academic Press, San Diego. 383–391.

Horiike, K., H. Tojo, T. Yamano, and M. Nozaki. 1983. Interpretation of the stokes radius of macromolecules determined by gel filtration chromatography. *J. Biochem. (Tokyo).* 93:99–106.

Ikura, M., T. Hiraoki, K. Hikichi, T. Mikuni, M. Yazawa, and K. Yagi. 1983. Nuclear magnetic resonance studies on calmodulin: calcium-induced conformational change. *Biochemistry.* 22:2573–2579.

Ikura, M., T. Hiraoki, K. Hikichi, O. Minowa, H. Yamaguchi, M. Yazawa, and K. Yagi. 1984. Nuclear magnetic resonance studies on calmodulin: Ca^{2+}-dependent spectral change of proteolytic fragments. *Biochemistry.* 23:3124–3128.

Ikura, M., O. Minowa, and K. Hikichi. 1985. Hydrogen bonding in the carboxyl-terminal half-fragment 78–148 of calmodulin as studied by two-dimensional nuclear magnetic resonance. *Biochemistry.* 24: 4264–4269.

Ikura, M., S. Spera, G. Barbato, L. E. Kay, M. Krinks, and A. Bax. 1991. Secondary structure and side-chain ^{1}H and ^{13}C resonance assignments of calmodulin in solution by heteronuclear multidimensional NMR spectroscopy. *Biochemistry.* 30:9216–9228.

Johnson, M. L., and S. G. Frasier. 1985. Nonlinear least-squares analysis. *Methods Enzymol.* 117:301–342.

Kataoka, M., J. F. Head, A. Persechini, R. H. Kretsinger, and D. M. Engelman. 1991a. Small-angle X-ray scattering studies of calmodulin mutants with deletions in the linker region of the central helix indicate that the linker region retains a predominantly α-helical conformation. *Biochemistry.* 30:1188–1192.

Kataoka, M., J. F. Head, B. A. Seaton, and D. M. Engelman. 1989. Melittin binding causes a large calcium-dependent conformational change in calmodulin. *Proc. Natl. Acad. Sci. USA.* 86:6944–6948.

Kataoka, M., J. F. Head, T. Vorherr, J. Krebs, and E. Carafoli. 1991b. Small-angle x-ray scattering study of calmodulin bound to two peptides corresponding to parts of the calmodulin-binding domain of the plasma membrane Ca^{2+} pump. *Biochemistry.* 30:6247–6251.

Kita, Y., T. Arakawa, T. Lin, and S. N. Timasheff. 1994. Contribution of the surface free energy perturbation to protein-solvent interactions. *Biochemistry.* 33:15178–15189.

Klee, C. B., and P. Cohen. 1988. The calmodulin-regulated protein phosphatase. *In* Calmodulin. P. Cohen and C. B. Klee, editors. Elsevier, New York. 225–248.

Klee, C. B., and T. C. Vanaman. 1982. Calmodulin. *Adv. Protein Chem.* 35:213–321.

Klevit, R. E., D. C. Dalgarno, B. A. Levine, and R. J. P. Williams. 1984. ^{1}H-NMR studies of calmodulin: the nature of the Ca^{2+}-dependent conformational change. *Eur. J. Biochem.* 139:109–114.

Kraulis, P. J. 1991. MOLSCRIPT: a program to produce both detailed and schematic plots of protein structures. *J. Appl. Crystallogr.* 24:946–950.

Kretsinger, R. H. 1992. The linker of calmodulin: to helix or not to helix. *Cell Calcium.* 13:363–376.

Kretsinger, R. H., and C. E. Nockold. 1973. Carp muscle calcium-binding protein. *J. Biol. Chem.* 215:3313–3326.

Kuboniwa, H., N. Tjandra, S. Grzesiek, H. Ren, C. B. Klee, and A. Bax. 1995. Solution structure of calcium-free calmodulin. *Nature Struct. Biol.* 2:768–776.

Kung, C., R. R. Preston, M. E. Maley, K.-Y. Ling, J. A. Kanabrocki, B. R. Seavey, and Y. Saimi. 1992. In vivo *Paramecium* mutants show that calmodulin orchestrates membrane responses to stimuli. *Cell Calcium.* 13:413–425.

Kuntz, I. D., and W. Kauzmann. 1974. Hydration of proteins and polypeptides. *Adv. Protein Chem.* 28:239–338.

Kupke, D. W. 1986. Sequential volume changes on a small sample by density. *Anal. Biochem.* 158:463–468.

Kupke, D. W., and B. S. Shank. 1989. Volume change for calcium(II) to tetracarboxylate sequestrants: relevance to calcium binding proteins. *J. Phys. Chem.* 93:2101–2106.

LaPorte, D. C., B. M. Wierman, and D. R. Storm. 1980. Calcium-induced exposure of a hydrophobic surface on calmodulin. *Biochemistry.* 19: 3814–3819.

Laskowski, R. A., M. W. MacArthur, D. S. Moss, and J. M. Thornton. 1993. PROCHECK: a program to check the stereochemical quality of protein structures. *J. Appl. Crystallogr.* 26:283–291.

Laurent, T. C., and J. Killander. 1964. A theory of gel filtration and its experimental verification. *J. Chromatogr.* 14:317–330.

Le Maire, M., A. Viel, and J. V. Møller. 1989. Size exclusion chromatography and universal calibration of gel columns. *Anal. Biochem.* 177: 50–56.

Lu, K. P., and A. R. Means. 1993. Regulation of the cell cycle by calcium and calmodulin. *Endocr. Rev.* 14:40–58.

Lu, K. P., S. A. Osmani, A. H. Osmani, and A. R. Means. 1993. Essential roles for calcium and calmodulin in G_2/M progression in *Aspergillus nidulans*. *J. Cell Biol.* 115:426 (Abstr.).

Matsushima, N., Y. Izumi, T. Matsuo, H. Yoshino, T. Ueki, and Y. Miyake. 1989. Binding of both Ca^{2+} and mastoparan to calmodulin induces a large change in the tertiary structure. *J. Biochem. (Tokyo).* 105:883–887.

Maune, J. F., C. B. Klee, and K. Beckingham. 1988. Calmodulin point mutations which affect Ca^{2+}-binding and calcineurin activation. *J. Cell Biol.* 107:287a. (Abstr.)

Maune, J. F., C. B. Klee, and K. Beckingham. 1992. Ca^{2+} binding and conformational change in two series of point mutations to the individual Ca^{2+}-binding sites of calmodulin. *J. Biol. Chem.* 267:5286–5295.

Mehler, E. L., J.-L. Pascual-Ahuir, and H. Weinstein. 1991. Structural dynamics of calmodulin and tryponin C. *Protein Eng.* 4:625–637.

Ogston, A. G. 1958. The spaces in a uniform random suspension of fibres. Trans. Faraday Soc. 54:1754–1757.

Oncley, J. L. 1941. Evidence from physical chemistry regarding the size and shape of protein molecules from ultra-centrifugation, diffusion, viscosity, dielectric dispersion, and double refraction of flow. *Ann. N.Y. Acad. Sci.* 41:121–150.

Pascual-Ahuir, J.-L., E. L. Mehler, and H. Weinstein. 1991. Calmodulin structure and function: implication of arginine in the compaction related to ligand binding. *Mol. Eng.* 1:231–247.

Pedigo, S., and M. A. Shea. 1995. Quantitative endoproteinase GluC footprinting of cooperative Ca^{2+} binding to calmodulin: proteolytic susceptibility of E31 and E87 indicates interdomain interactions. *Biochemistry.* 34:1179–1196.

Perrin, F. 1936. Mouvement Brownien d'un ellipsoide (II). Rotation libre et depolarization des fluorescences. Translation et diffusion de molécules ellipsoidales. *J. Phys. Radium.* 7:1–11.

Persechini, A., and R. H. Kretsinger. 1988. The central helix of calmodulin functions as a flexible tether. *J. Biol. Chem.* 263:12175–12178.

Pharmacia Biotech. 1996. Gel Filtration Calibration Kit Instruction Manual for Protein Molecular Weight Determinations by Gel Filtration. Catalog no. 17-0441-01. Pharmacia Biotech, Piscataway, NJ.

Pharmacia LKB Biotechnology. 1991. Gel Filtration Principles and Methods. Pharmacia LKB Biotechnology, Uppsala, Sweden.

Porath, J. 1963. Some recently developed fractionation procedures and their application to peptide and protein hormones. *J. Pure Appl. Chem.* 6:233–244.

Potschka, M. 1987. Universal calibration of gel permeation chromatography and determination of molecular shape in solution. *Anal. Biochem.* 162:47–64.

Putkey, J. A., G. R. Slaughter, and A. R. Means. 1985. Bacterial expression and characterization of proteins derived from the chicken calmodulin cDNA and a calmodulin processed gene. *J. Biol. Chem.* 260: 4704–4712.

Rasmussen, C. D., and A. R. Means. 1989. Calmodulin is required for cell-cycle progression during G_1 and mitosis. *EMBO J.* 8:73–82.

Rasmussen, C. D., R. L. Means, K. P. Lu, G. S. May, and A. R. Means. 1990. Characterization and expression of the unique calmodulin gene of *Aspergillus nidulans*. *J. Biol. Chem.* 265:13767–13775.

Seamon, K. B. 1980. Calcium- and magnesium-dependent conformational states of calmodulin as determined by nuclear magnetic resonance. *Biochemistry.* 19:207–215.

Seaton, B. A., J. F. Head, D. M. Engelman, and F. M. Richards. 1985. Calcium-induced increase in the radius of gyration and maximum dimension of calmodulin measured by small-angle x-ray scattering. *Biochemistry.* 24:6740–6743.

Shea, M. A., A. S. Verhoeven, and S. Pedigo. 1996. Calcium-induced interactions of calmodulin domains revealed by quantitative thrombin footprinting of Arg37 and Arg106. *Biochemistry.* 35:2943–2957.

Siegel, L. M., and K. J. Monty. 1966. Determination of molecular weights and frictional ratios of proteins in impure systems by use of gel filtration and density gradient centrifugation. Application to crude preparations of sulfite and hydroxylamine reductases. *Biochim. Biophys. Acta.* 112: 346–362.

Small, E. W., and S. R. Anderson. 1988. Fluorescence anisotropy decay demonstrates calcium-dependent shape changes in photo-cross-linked calmodulin. *Biochemistry.* 27:419–428.

Sorensen, B. R., and M. A. Shea. 1995. Mutational perturbation of calmodulin structure. *Biophys. J.* 68:A403.

Squire, P. G. 1964. A relationship between the molecular weights of macromolecules and their elution volumes based on a model for Sephadex gel filtration. *Arch. Biochem. Biophys.* 107:471–478.

Squire, P. G., and M. E. Himmel. 1979. Hydrodynamics and protein hydration. *Arch. Biochem. Biophys.* 196:165–177.

Stafford, W. F., and T. M. Schuster. 1995. Hydrodynamic methods. *In* Introduction to Biophysical Methods for Protein and Nucleic Acid Research. Academic Press, San Diego. 111–145.

Strynadka, N. C. J., and M. N. G. James. 1989. Crystal structures of the helix-loop-helix calcium-binding proteins. *Annu. Rev. Biochem.* 58: 951–998.

Tabor, S., and C. C. Richardson. 1985. A bacteriophage T7 RNA polymerase/promoter system for controlled exclusive expression of specific genes. *Proc. Natl. Acad. Sci. USA.* 82:1074–1078.

Tanford, C., Y. Nozaki, A. Reynolds, and S. Makino. 1974. Molecular characterization of proteins in detergent solutions. *Biochemistry.* 13: 2369–2376.

Taylor, D. A., J. S. Sack, J. F. Maune, K. Beckingham, and F. A. Quiocho. 1991. Structure of a recombinant calmodulin from *Drosophila melanogaster* refined at 2.2-Å resolution. *J. Biol. Chem.* 266:21375–21380.

Tjandra, N., H. Kuboniwa, H. Ren, and A. Bax. 1995. Rotational dynamics of calcium-free calmodulin studied by ^{15}N-NMR relaxation measurements. *Eur. J. Biochem.* 230:1014–1024. (Abstr.)

Török, K., A. N. Lane, S. R. Martin, J.-M. Janot, and P. M. Bayley. 1992. Effects of calcium binding on the internal dynamic properties of bovine brain calmodulin, studied by NMR and optical spectroscopy. *Biochemistry.* 31:3452–3462.

Urbauer, J. L., J. H. Short, L. K. Dow, and A. J. Wand. 1995. Structural analysis of a novel interaction by calmodulin: high affinity binding of a peptide in the absence of calcium. *Biochemistry.* 34:8099–8109.

Wang, C. A. 1989. pH-dependent conformational changes of wheat germ calmodulin. *Biochemistry.* 28:4816–4820.

Wang, C.-L. A. 1985. A note on Ca^{2+} binding to calmodulin. *Biochem. Biophys. Res. Commun.* 130:426–430.

Warshaw, H. S., and G. K. Ackers. 1971. Molecular sieve studies of interacting protein systems. VIII. Critical evaluation of the equilibrium sturation technique using stacked gel columns. *Anal. Biochem.* 42: 405–421.

Weinstein, H., and E. L. Mehler. 1994. Ca^{2+}-binding and structural dynamics in the functions of calmodulin. *Annu. Rev. Physiol.* 56:213–236.

Yao, Y., C. Schöneich, and T. C. Squier. 1994. Resolution of structural changes associated with calcium activation of calmodulin using frequency domain fluorescence spectroscopy. *Biochemistry.* 33: 7797–7810.

Yazawa, M., F. Matsuzawa, and K. Yagi. 1990. Inter-domain interaction and the structural flexibility of calmodulin in the connecting region of the terminal two domains. *J. Biochem. (Tokyo).* 107:287–291.

Yoshino, H., O. Minari, N. Matsushima, T. Ueki, Y. Miyake, T. Matsuo, and Y. Izumi. 1989. Calcium-induced shape change of calmodulin with mastoparan studied by solution x-ray scattering. *J. Biol. Chem.* 264: 19706–19709.

Yoshino, H., M. Wakita, and Y. Izumi. 1993. Calcium-dependent changes in structure of calmodulin with substance P. *J. Biol. Chem.* 268: 12123–12128.

Zhang, M., T. Tanaka, and M. Ikura. 1995. Calcium-induced conformational transition revealed by the solution structure of apo calmodulin. *Nature Struct. Biol.* 2:758–767.